DOI 10.1007/s11182-020-02120-5
Russian Physics Journal, Vol. 63, No. 6, October, 2020 (Russian Original No. 6, June, 2020)

THE EFFECT OF IRRADIATION OF A TITANIUM ALLOY OF THE Ti–6Al–4V–H SYSTEM WITH PULSED ELECTRON BEAMS ON ITS CREEP

G. P. Grabovetskaya,[1] E. N. Stepanova,[2] I. P. Mishin,[1] and O. V. Zabudchenko[1] UDC 539.376:559.424

Comparative studies of the effect of pulsed electron beam irradiation of the Ti–6Al–4V *titanium alloys with the contents of hydrogen of 0.002 wt.% (VT6 alloy) and 0.23 wt.% (VT6–0.23H alloy) on their structure and peculiar creep behavior are performed at a temperature of 723 K within the range of creep rates* 10^{-7}*–*10^{-5} s^{-1}*. It is found out that irradiation of the VT6 and VT6–0.23H alloy samples with electron beams in the no-melting mode neither changes nor increases their steady-state creep. It is shown that formation of a modified surface layer during electron beam irradiation in the melting mode gives rise to a decrease in the steady-state creep rate in the VT6 alloy and its increase in the VT6–0.23H alloy. It is demonstrated that the dependence of the steady-state creep of the VT6 alloy on the stress before and after pulsed electron beam irradiation is satisfactorily described by the creep power law. The presence of hydrogen in a solid solution in the VT6–0.23H alloy violates the creep power law. The physical causes for the high values of a stress sensitivity index and an effective creep activation energy of the VT6 and VT6–0.23H alloys are discussed.*

Keywords: titanium alloy, hydrogen, pulsed electron beam, creep.

INTRODUCTION

The methods of surface treatment relying on the use of electron beams offer an improvement of wear resistance, corrosion resistance and dynamic strength of metallic materials [1, 2]. Their impact, however, causes steep temperature and stress gradients in the irradiated material, which, depending on the irradiation mode, can result in accumulation of defects in the surface layer, redistribution of impurities and formation of metastable phases [3–5]. Note that the presence of hydrogen in the material can significantly affect the phase composition and the type of defects formed in the course of irradiation. In particular, the presence of hydrogen in the alloys based on titanium, zirconium and other elements decreases the allotropic transformation temperature and favors the formation of metastable phases [6–8]. It is also known that hydrogen can induce the formation of defects in materials and can actively interact with the already available structure defects [9]. The surface structure having a high density of defects and containing metastable phases can turn out to be unstable at the elevated operating temperatures. The modified layer instability to a temperature impact in the presence of hydrogen would be especially pronounced at low deformation rates typical for creep, where the role of diffusion and diffusion-controlled processes in the development of plastic strain is especially important. On the other hand, there has been practically no discussion of the influence of electron beam irradiation of metallic materials on their creep in the available literature.

The purpose of this work is to study the effect of electron beam irradiation of a Ti–6Al–4V–H titanium alloy on the regularities of its creep.

---

[1] Institute of Strength Physics and Materials Science of the Siberian Branch of the Russian Academy of Sciences, Tomsk, Russia, e-mail: grabg@ispms.tsc.ru; mip@ispms.tsc.ru; lekalune@mail.ru; [2] National Research Tomsk Polytechnic University, Tomsk, Russia, e-mail: enstepanova@tpu.ru. Translated from Izvestiya Vysshikh Uchebnykh Zavedenii, Fizika, No. 6, pp. 30–36, June, 2020. Original article submitted February 12, 2020.

EXPERIMENTAL MATERIAL AND PROCEDURE

The experiments were performed using a two-phase (α+β) Ti–6Al–4V titanium alloy with the following contents of the alloying elements: Al – 5.9 wt.% and V – 3.9 wt.%. The content of hydrogen in the as-received alloy (referred to here as the VT6 alloy) does not exceed 0.002 wt.%. The samples were irradiated with electron beams at the energy densities 5 and 12 J/cm^2 in a SOLO facility [10] in an argon atmosphere at a residual pressure of 0.02 Pa, using three pulses with a pulse frequency of 0.3 s^{-1} an a pulse duration of 50 μs. During electron beam irradiation at the energy density of 12 J/cm^2 the surface layer undergoes high-rate melting and high-rate crystallization (surface melting mode). Electron beam irradiation at the energy density of 5 J/cm^2 does not cause any surface melting (no-melting mode).

Before irradiation part of the specimens was hydrogenated to a concentration of 0.23±0.01 wt.% H (referred to as the VT6–0.23H alloy). The specimens were hydrogenated by annealing in a hydrogen medium in a PCIM high-vacuum facility of a Siverst type at a temperature of 773 K and a pressure of 1 atm. The concentration of hydrogen was measured with a RHEN 602 gas analyzer to an accuracy of 0.0001%.

The structure of the alloy samples before and after irradiation was investigated in the optical (AXIOVERT-200MAT) and transmission electron (JEM-2100) microscopes. The dimensions of the structural elements were measured on the micrographs using the linear intercept method.

The phase compositions of the alloys were determined by the method of X-ray diffraction analysis in a Shimadzu XRD-7000 diffractometer in a CuK_α radiation source. The diffraction patterns were interpreted using the PowderCell software program. The dislocation density and the value of lattice microdeformation in the α-titanium were determined by a standard XRD analysis from the peak broadening at half of the maximum intensity (FWHM) using the Cauchy approximation [11, 12]. In order to separate the contributions from the coherently scattering regions and lattice microdeformation into the peak broadening, we used the diffraction maxima of the (101) and (103) planes.

The tension and creep tests were performed at a temperature of 723 K in a PV-3012M modernized testing machine in vacuum at a residual pressure of 10^{-2} Pa using flat dumb bell samples with the gauging sections of 5×1.5×1 mm. The samples were cut from the work pieces by the electrospark method. The sample surfaces were ground and electrolytically polished. The tests on the alloy creep were performed at a constant tensile loading within the range of rates 10^{-7}– 10^{-5} s^{-1}. The elongation of the samples was measured in a KM-6 optical cathetometer accurately within ±5 μm. The value of the effective creep activation energy (Q_c) was determined by a standard temperature-jump method via increasing/decreasing the temperature by 10 K. The values of Q_c were calculated by the formula [13]

$$Q_c = R\ln(\dot{\varepsilon}_2/\dot{\varepsilon}_1)/(1/T_1 - 1/T_2)\,, \tag{1}$$

where $\dot{\varepsilon}_1$ and $\dot{\varepsilon}_2$ are steady-state creep rates before and after the temperature measurement, respectively, R is the gas constant, T_1 and T_2 are the absolute temperatures.

RESULTS AND DISCUSSION

The as-received (initial state) VT6 alloy with a hydrogen content of ~0.002 wt.% has a polycrystalline structure consisting of non-equiaxed grains of α-titanium with β-titanium interlayers between them (Fig. 1*a*).

In the β-interlayers, there are plates and particles of the α-phase. The grain size in the α-phase varies within the range between 5–15 μm, and that of interlayers – within 1–3 μm. The β-phase content in the alloy is as low as 6 vol.% (Fig. 2*a*, Curve *1*). The optical and electron-microscopy examinations of the structure demonstrated that the hydrogenation of the alloy to 0.23 wt.% does not change the average size of the α-phase grains of the VT6 alloy, but results in a larger volume fraction of the β-phase up to (14±2) vol.% (Fig. 2*b*, Curve *1*). It should be noted that the number of α-phase precipitates in the β-phase interlayers becomes smaller, and the β-phase lattice parameter increases from 0.3224 to 0.330 nm (Fig. 2*b*, Curve *1*). The latter circumstance indicates a smaller content of vanadium in the β-phase volume [14].

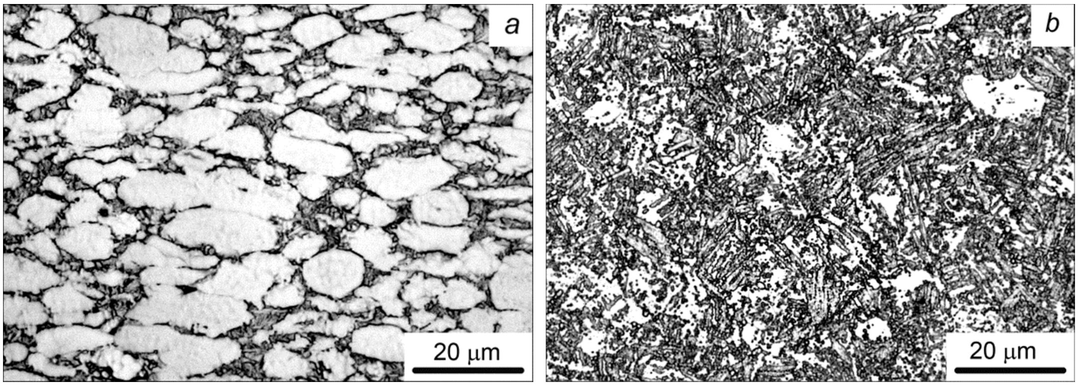

Fig. 1. Microstructure of the VT6 alloy before (*a*) and after (*b*) its irradiation with a pulsed electron beam in the surface melting mode.

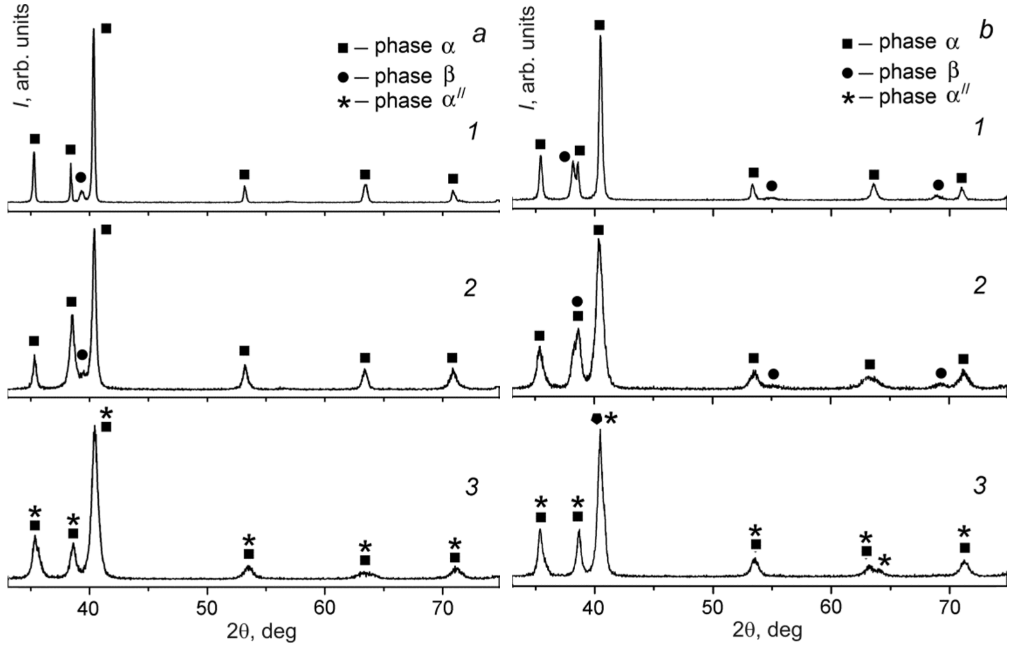

Fig. 2. Diffraction pattern areas of VT6 (*a*) and VT6–0.23H (*b*) alloys before and after (*b*) its irradiation with a pulsed electron beam in the surface melting mode: Curve *1* – initial state, Curve *2* – after irradiation in the no-melting mode, Curve *3* – after irradiation in the surface-melting mode.

An irradiation of the VT6 and VT6–0.23H alloys with a pulsed electron beam in the no-melting mode does not change their structure, phase composition and hydrogen concentration. On the other hand, the X-ray peaks (Fig. 2*a*, *b*, Curves *2*) in the diffraction patterns obtained from the surface layers of both alloys irradiated with pulsed electron beams are broadened, which indicates an increase in the surface layer stresses. According to the estimates based on the broadened FWHM peaks, the crystal lattice microdistortions ($\Delta\varepsilon$) of the α-phase titanium in the VT6 and VT6–0.23H alloys after irradiation with electron beams in the no-melting mode are found to be $2.8\cdot10^{-3}$ and $4.8\cdot10^{-3}$, respectively, and the dislocation densities (ρ) – $2.8\cdot10^{13}$ and 10^{14} m^{-2}, respectively. In the main bulk of the irradiated VT6 and VT6–

TABLE 1. Mechanical Properties of VT6 and VT6–0.23H alloys at 723 K before and After Electron Beam Irradiation

Material	E, J/cm^2	$\sigma_{0.2}$, MPa	σ_{UTS}, MPa	ε_B, %	δ, %
VT6	0	569	636	8	26
VT6–0.23H		580	707	5	19
VT6	5	573	620	8	24
VT6 –0.23H		587	689	6	20
VT6	12	589	655	9	23
VT6 –0.23H		572	680	7	22

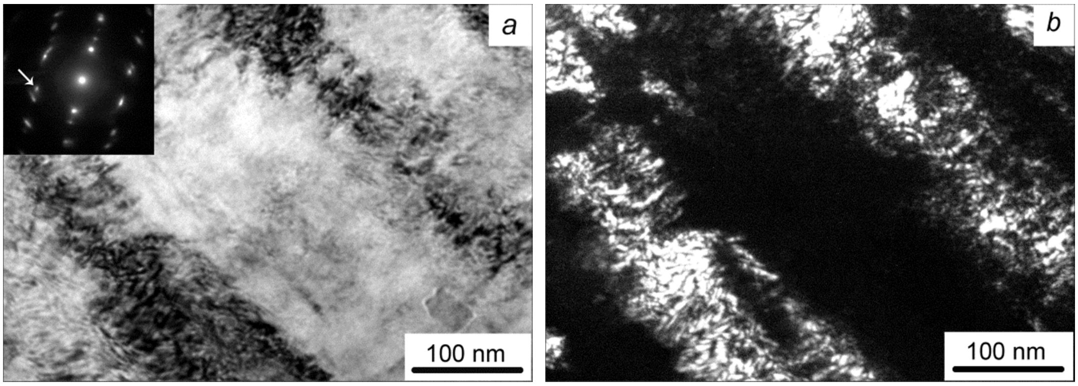

Fig. 3. TEM image of the surface layer structure of the VT6 alloy after its irradiation with a pulsed electron beam in the surface melting mode: *a* – bright-field image with a respective microdiffraction pattern; *b* – dark-field image in the 103 α''-phase reflection.

0.23H samples the values of $\Delta\varepsilon$ and ρ do not practically change and are as follows: $\Delta\varepsilon$ – 10^{-3} and $1.6\cdot10^{-3}$ and ρ – $4\cdot10^{12}$ and $1.7\cdot10^{13}$ m^{-2}, respectively.

After irradiation of the VT6 and VT6–0.23H alloy samples with pulsed electron beams in the surface melting mode, in their surface layer 10–12 μm in thickness a polycrystalline structure is formed with the equiaxed grains whose size is 5–10 μm. A platelet structure is observed in the bulk of these grains (Fig. 1*b*). The electron-microscopy examinations demonstrated that the platelet structure of the modified layer consists of the plates of different degrees of dispersion. In the plates with a transverse size of 100–300 nm there are platelet-shape precipitates whose width is 10–20 nm (Fig. 3). An interpretation of the X-ray diffraction patterns demonstrated that these plates represent the $\alpha(\alpha')$- and α''-phases of titanium. The XRD investigations validate the phase composition changes in the modified layers of the VT6 and VT6–0.23H alloys. There are no X-ray peaks from the β-phase, and the X-ray peaks from the α-phase become asymmetrical (Fig. 2, Curves *3*) in the XRD patterns from the modified layers of the samples of both alloys irradiated with pulsed electron beams in the surface melting mode. This asymmetry of X-ray peaks is due to the α''-phase formation. In addition to the phase composition change in the surface layer of the VT6–0.23H alloy as a result of its irradiation with an electron beam in the surface melting mode, there is a decrease in the hydrogen concentration from about 0.23 to 0.2 wt.%.

Table 1 presents the values of strength and plastic characteristics of the VT6 and VT6–0.23H alloys in different states during tension at a temperature of 723 K. It is clear from Table 1 that hydrogenation of the sample to a concentration of 0.23 wt.% results in higher values of the ultimate tensile strength (σ_{UTS}) of the VT6 alloy at practically the same yield stress values ($\sigma_{0.2}$) and lower values of homogeneous strain (ε_{UTS}) and elongation to fracturet (δ). Electron beam irradiation of the VT6 and VT6–0.23H alloys under the modes used in this work only slightly affects their strength and plasticity characteristics during tension.

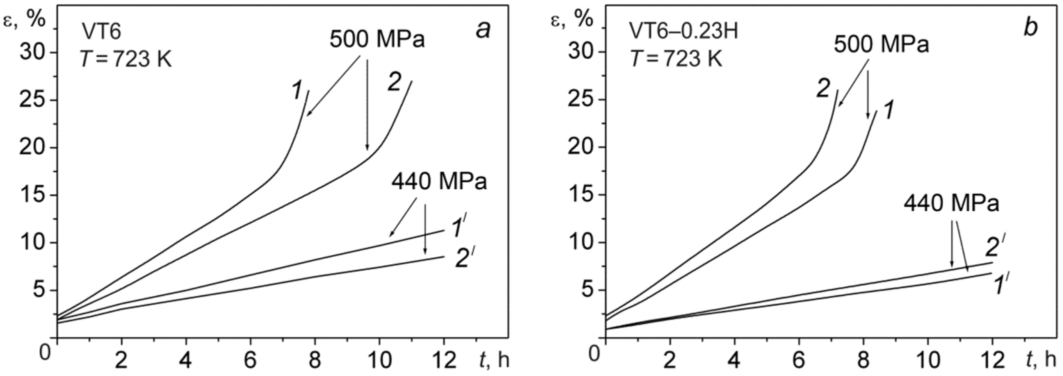

Fig. 4. Creep curves at 723 K for the VT6 (a) and VT6–0.23H (*b*) alloys in the nonirradiated states (Curves *1* and *1*′) and after irradiation in the surface melting mode (Curves *2* and *2*′).

Figure 4 presents the creep curves for the VT6 and VT6–0.23H alloys at a temperature of 723 K. It is evident that in the general case there are two creep stages: steady-state and accelerated creep. A comparison of these curves demonstrates that hydrogenation of theVT6 alloy to a concentration of 0.23 wt.% gives rise to a decrease in the steady-state creep rate accompanied by a decrease in the steady-state creep duration and time to fracture (Fig. 4*a* and *b*). This effect of hydrogenation on creep could be, on the one hand, attributed to hardening of the β-phase, and hydrogen diffusion, on the other hand. Possessing high diffusion mobility, hydrogen can be redistributed in the alloy bulk under the action of elastic stress fields, forming hydrogen-accumulation areas and pores in the stressed regions, which results in strain localization and early fracture [15, 16]. This assumption is validated by the hydrogen concentration measurements in different areas of a nonirradiated sample of the VT6–0.23H alloy after its creep at 773 K. Specifically, in the vicinity of the fracture site the hydrogen concentration increased from 0.23 to 0.27 wt.%. The vacancies and hydrogen-vacancy complexes forming in the volume of the hydride-forming alloys as a result of hydrogenation, as shown in [9, 17], can also exert their influence on the creep behavior in the VT6–0.23H alloy.

Pulsed electron beam irradiation does not practically change the shapes of the creep curves of the VT6 and VT6–0.23H alloys, but can affect the rate and duration of the steady-state creep stage. For instance, an irradiation of the VT6 alloy in the surface melting mode results in a 20–30% decrease in the steady-state creep rate and a factor of 1.3–1.5 increase in the steady-state creep duration (Fig. 4*a*), but in the no-melting mode does not affect these creep characteristics. A lower creep rate of the VT6 alloy observed after its irradiation in the surface melting mode is likely to be caused by increased shear stability of the surface layer due to the platelet structure formation [18].

An irradiation of the VT6–0.23H alloy in both regimes gives rise to a 10–20% increase in the steady-state creep rate (Fig. 4*b*). This could be due to an increased density of such defects as vacancy and hydrogen-vacancy complexes, and the formation of cluster-hydrogen complexes [19–21], which can negatively affect creep resistance of the alloy. A higher steady-state creep rate observed in the VT6–0.23H alloy after its irradiation in the melting mode could be due to not only defect formation, but also a lower hydrogen concentration in the β-phase of titanium and, as a consequence, a decrease in its strength characteristics.

An investigation of the dependence of the steady-state creep rate in the VT6 alloy before and after irradiation at 723 K on the applied stress demonstrated that these relationships in the log-log coordinates have a linear character (Fig. 5*a*). This indicates that creep of the VT6 alloys before and after their irradiation under the selected experimental conditions is described by a well-known creep power law [19]:

$$\dot{\varepsilon} = A\sigma^n \exp(Q / RT)\,, \tag{2}$$

where $\dot{\varepsilon}$ is the steady-state creep rate, n is the index of stress sensitivity, A is the constant, Q_c is the effective creep activation energy, R is the universal gas constant, T is the temperature.

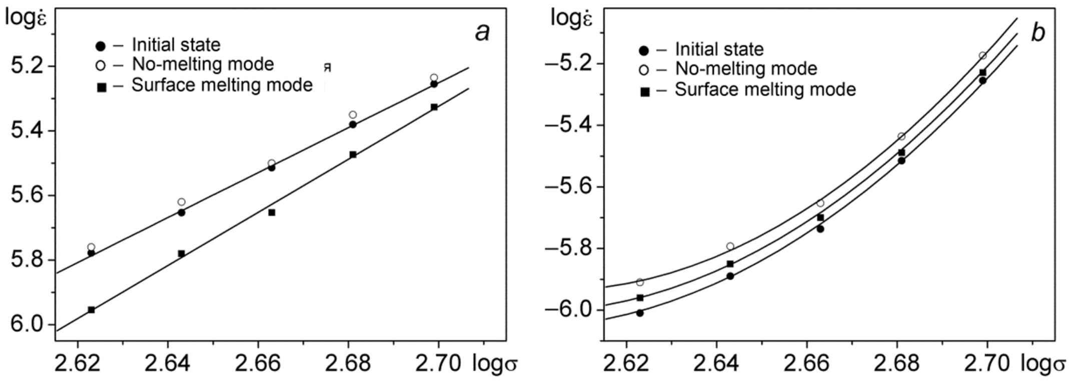

Fig. 5. Dependence of the steady-state creep rate on stress in the VT6 (*a*) and VT6-0.23H (*b*) alloys at a temperature of 723 K.

According to equation (2), the mechanism controlling creep in the VT6 alloy can be determined using the values of indices *n* and Q_c. It follows from the tilt of the curves in Fig. 5*a* that for the VT6 alloy in its initial state and after irradiation in the no-melting mode the value of index *n* is ~7. After electron beam irradiation in the surface melting mode, its value increases to ~8.2. The values of Q_c for the VT6 alloy in the states before and after irradiation, which were determined by the method of temperature jump, were found to be (279±20) and (302±20) kJ/mol, respectively. It is well known that [18, 19] that creep in titanium in the coarse- and fine-grained states under the conditions used in this study ($T < 0.4T_{\mathrm{melt}}$ and $\dot{\varepsilon} = 10^{-6}$–$10^{-5}$ s^{-1}) occurs by the motion (glide and climb) of dislocations. Note that the value of $n = 4.3$ and the value of Q_c is close to that of the activation energy of the bulk self-diffusion of titanium [18, 19]. The values of *n* and Q_c obtained in this work for the VT6 experimental alloy are much higher than those corresponding to the dislocation-induced creep. According to the authors of [20, 21], high values of indices *n* and Q_c during creep can indicate the presence of a threshold stress, below which no creep is observed, rather than a change in the principal mechanism of creep and the process controlling it. Given the threshold stress, the dependence of the steady-state creep rate on stress and temperature for the VT6 experimental alloy can be given by

$$\dot{\varepsilon} = A(\sigma - \sigma_0)^n \exp(-Q/RT)\,, \tag{3}$$

where σ_0 is the threshold stress, $n = 4.3$.

Figure 6 presents the dependences of $\dot{\varepsilon}^{1/n}$ on σ for the VT6 alloys in the states before and after irradiation at $n = 4.3$. An extrapolation of these curves to a zero creep rate showed that, under the experimental conditions of this study for the VT6 alloy before and after irradiation, the threshold stresses (σ_0) are ~185 and ~220 MPa, respectively.

Using equations (3) and (4) to calculate Q_c, we obtain its values for the nonirradiated and irradiated states of the VT6 alloy: (162±20) and (149±20) kJ/mol, respectively. These values of Q_c are close to each other and to the value of the activation energy of volume self-diffusion of titanium which, according to the literature data [18–21], is equal to 122– 169 kJ/mol. Therefore, pulsed electron beam irradiation of the VT6 titanium alloy does not change its principal creep mechanism under the conditions studied in this work. A most probable creep mechanism is the dislocation-induced creep. A decrease in the creep rate in the VT6 alloy observed after its irradiation in the surface melting mode is likely to be caused by an increased shear stability of the surface layer due to the platelet structure formation [22].

An investigation of the dependence of the steady-state creep on the applied loading stress in the VT6–0.23H alloy before and after irradiation using both regimes showed that at 723 K these dependences in the log-log coordinates are not linear (Fig. 5*b*). This indicates a violation of the power law during creep in the VT6–0.23H alloy containing hydrogen in a solid solution. It is seen in Fig. 5*b* that the index *n* increases with the rise in the applied stress. This behavior of index *n* seems to be associated with the hydrogen capability to distribute in the sample volume under stress. It is known [23] that at a given temperature the flux of hydrogen increases with the tensile stress. Therefore, as the

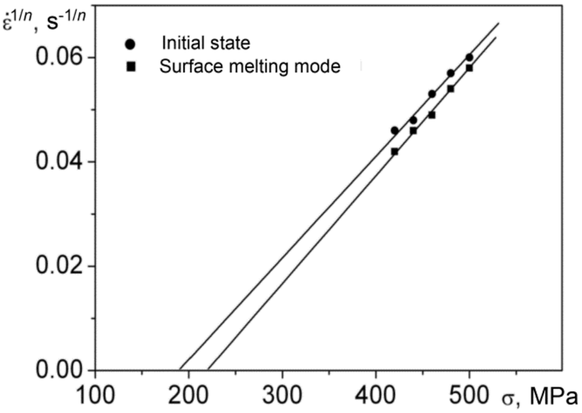

Fig. 6. Dependence of the value of $\dot{\varepsilon}^{1/n}$ of the VT6 and VT6–0.23H alloys on stress at a temperature of 723 K.

tensile stress increases the rate of formation of the hydrogen-accumulation areas and pores in the sample regions with the highest stress, which would give rise to a decrease in its creep resistance.

SUMMARY

It has been shown that irradiation of the VT6 and VT6–0.23H alloys with pulsed electron beams in the no-melting modes does not change their structure morphology. As a result of irradiation in the melting mode, platelet α+α''-structure with the transverse size of the plates within 10–300 nm is formed in the 10–12 μm wide surface layers of the VT6 and VT6–0.23H alloys.

An irradiation of the VT6 alloy in the melting mode favors a decrease in the steady-state rate by 20–30% and an increase in the duration of this stage 1.3–1.5 factors. An irradiation of the VT6–0.23H alloy with pulsed electron beams in the no-melting and melting modes results in a 10–20% increase in the steady-state creep rate. This is supposed to be due to the formation of vacancy and cluster-hydrogen complexes in the alloy during its irradiation and to partial degassing of hydrogen from the alloy.

The dependence of the creep rate on stress in the VT6 alloy before and after irradiation at 723 K is satisfactorily described by the power law of creep. It should be noted that the principal creep mechanism is dislocation motion controlled by the volume self-diffusion of titanium. The presence of hydrogen in the VT6–0.23H alloy in a solid solution gives rise to a violation of the power law of creep.

The work was carried out with the financial support of the Russian Foundation for Basic research (grant No. 18-08-00158) and within the framework of the Government Research Assignment for ISPMS SB RAS, Project No. III.23.2.2 using the equipment of the TSU Materials Science Center for Collective Use.

REFERENCES

1. Yu. V. Baranov, O. A. Troitskii, Yu. S. Abramov, *et al.*, Principal Physics of Electric Discharge Machining and Electroplastic Treatment and New Materials [in Russian], MGIU, Moscow (2001).
2. Y. J. Liu, H. L. Wang, W. T. Hou, *et al.*, Acta Mater., **113**, 56–67 (2016).
3. Иванов Yu. F. Ivanov, A. A. Klopotov, A. I. Potekaev, *et al.*, Russ. Phys. J., **60**, No. 1, 175–180 (2017).
4. X. D. Zhang, S. Z. Hao, X. N. Li, *et al.*, Appl. Surf. Sci., **257**, No. 13, 5899–5902 (2011).
5. V. E. Panin, A. V. Panin, O. B. Perevalova, *et al.*, Physical Mesomechanics, **22(5)**, 345–354(2019).

6. Y. Fukai, The Metal-Hydrogen System: Basic Bulk Properties, Springer Science & Business Media (2006).
7. A. A. Ilyin, B. A. Kolachev, V. K. Nosov, *et al.*, A Hydrogen Technology of Titanium Alloys [in Russian], MISIS, Moscow (2002).
8. R. S. Laptev, A. M. Lider, Y. S. Bordulev, *et al.*, J. Alloys Compd., **645**, 193–195 (2015).
9. A. M. Lider, Positron Spectroscopy for Testing Microstructural Changes in the Metal-Hydrogen Systems [in Russian], Dissert. Dr. Tech. Sciences, NR TPU, Tomsk (2017).
10. N. N. Koval and Yu. F. Ivanov, Russ. Phys. J., **51**, No. 5, 505–516 (2008).
11. S. S. Gorelik, Yu. A. Skakov, and L. N. Rastorguev, X-ray Diffraction and Electron-Optical Analyses [in Russian], MISIS, Moscow (2002).
12. G. K. Williamson and R. E. Smallman, Phil. Mag., **1**, No. 1, 34–46 (1956).
13. F. Garofalo, Fundamentals of Creep Rupture in Metals, Mc Millan, New York (1965).
14. M. V. Maltsev and N. I. Kashnikov, Phys. Met. Metallogr., **45**, No. 2, 426–428 (1978).
15. B. A. Kolachev, Hydrogen Brittleness of Metals [in Russian], Metallurgiya, Moscow (1985).
16. E. N. Stepanova, G. P. Grabovetskaya, and O. V. Zabudchenko, Defect and Diffusion Forum, **385**, 212–217 (2018).
17. I. P. Mishin, G. P. Grabovetskaya, E. N. Stepanova, *et al.*, Russ. Phys. J., **62**, No. 5, 854–860 (2019).
18. E. V. Kollingz, Physical Metallurgy of Titanium Alloys [in Russian], Metallurgiya, Moscow (1988).
19. G. J. Frost and M. F. Ashby, Deformation Mechanism Maps, Pergamon Press (1982).
20. P. M. Sargent and M. F. Ashby, Scripta Metall., **16**, 1415–1422 (1982).
21. M. J. R. Barboza, E. A. C. Perez, M. M. Medeiros, *et al.*, Mater. Sci. Eng. A, **428**, 319–326 (2006).
22. W. J. Evans and G. F. Harrison, J. Mater. Sci., **18**, 3449–3455 (1983).
23. P. V. Geld, P. A. Ryabov, and E. S. Kodes, Hydrogen and Imperfections of Metal Structure [in Russian], Metallurgiya, Moscow (1979).